Glibenclamide Enhances Neurogenesis and Improves Long-term Functional Recovery after Transient Focal Cerebral Ischemia

Francisco J Ortega, PhD[1,2]; Jukka Jolkkonen, PhD[2]; Nicole Mahy, PhD[1]; Manuel J Rodríguez, PhD[1].

[1]*Unitat de Bioquímica i Biologia Molecular*, the *Facultat de Medicina*, the *Institut d'Investigacions Biomèdiques August Pi i Sunyer* (IDIBAPS), the *Universitat de Barcelona* and the *Centro de Investigación Biomédica en Red sobre Enfermedades Neurodegenerativas* (CIBERNED), Barcelona, Spain.

[2]Institute of Clinical Medicine – Neurology, University of Eastern Finland, Kuopio, Finland

Correspondence to: Dr. Francisco J Ortega

Unitat de Bioquímica i Biologia Molecular

Facultat de Medicina, UB

c/ Casanova 143

E-08036 Barcelona, SPAIN

Phone: +34 93 402 4525

FAX: +34 93 403 5882

e-mail: j.ortega@ub.edu

Acknowledgements

We thank Nanna Huuskonen, Laura Tolppanen, Anu Lipsanen and Dr. Tony Valente for their invaluable expert technical help. This work was supported by grants SAF2008-01902 from the Ministerio de Ciencia e Innovación, and by grant 2009SGR1380 from the Generalitat de

Catalunya (Autonomous Government), Spain; and Centre for International Mobility (CIMO), Finland. F.J.O. held a fellowship from Spanish Ministerio de Educación.

Disclosures

NM and MJR hold an EU patent (No. WO2006/000608). The other authors report no disclosures.

Running headline: Glibenclamide Enhances Neurogenesis after MCAO

ABSTRACT

Glibenclamide is neuroprotective against cerebral ischemia in rats. We studied whether glibenclamide enhances long-term brain repair and improves behavioral recovery after stroke. Adult male Wistar rats were subjected to transient middle cerebral artery occlusion (MCAO) for 90 min. A low dose of glibenclamide (total 0.6 μg) was administered i.v. 6, 12 and 24 h after reperfusion. We assessed behavioral outcome during a 30-day follow-up and animals were perfused for histologic evaluation. *In vitro* specific binding of glibenclamide to microglia increased after pro-inflammatory stimuli. *In vivo* glibenclamide was associated with increased migration of doublecortin-positive cells in the striatum toward the ischemic lesion 72 h after MCAO and reactive microglia expressed sulphonylurea receptor 1 (SUR1) and Kir6.2 in the striatum adjacent to the ventricle. One month after MCAO, glibenclamide also was associated with increased number of NeuN-positive and BrdU-positive neurons in the cortex and hippocampus, and enhanced angiogenesis in the hippocampus. Consequently, glibenclamide-treated MCAO rats showed improved performance in the limb-placing test on postoperative days 22 to 29 and in the cylinder and water-maze on postoperative test day 29. Therefore, acute blockade of SUR1 by glibenclamide enhanced long-term brain repair in MCAO rats, which was associated with improved behavioral outcome.

Key Words: angiogenesis, microglia, neural stem cells, neuroprotection, regeneration and recovery, brain ischemia

INTRODUCTION

The therapeutic potential of the administration of low doses of glibenclamide has been confirmed in different central nervous system (CNS) pathologies.[1] Particularly, in experimental stroke models it reduces cerebral edema and infarct volume, and decreases mortality.[2,3] In addition, this has been confirmed in stroke patients, where a retrospective study found that patients with diabetes mellitus taking glibenclamide that suffered an acute ischemic stroke had a better neurological outcome.[4]

Glibenclamide blocks the sulphonylurea receptor 1 (SUR1), the regulatory subunit of the K_{ATP}-[5] and the $NC_{Ca\text{-}ATP}$-channels,[1,6] which under ischemic conditions are expressed in neurons, astrocytes, oligodendrocytes, endothelial cells[1,7] and by reactive microglia.[8] It has been proposed that the blockade of the astroglial $NC_{Ca\text{-}ATP}$-channel by glibenclamide prevents cytotoxic edema after cerebral ischemia.[1,7] On the other hand, glibenclamide administration resulted in ameliorated reperfusion-derived oxidative stress and pro-inflammatory cytokine release in the rat hippocampus after cerebral ischemia in rats.[9] In line with this, our previous study demonstrated that glibenclamide administration at 6, 12 and 24 hours after reperfusion caused early neuroprotection and this was accompanied by a better neurological outcome.[8] Although recently Simard et al[10] showed an extended time window for glibenclamide treatment from 6 h to 10 h after onset of cerebral ischemia, and several studies point to a beneficial effect of glibenclamide to treat stroke, no previous studies have evaluated the long-term effects of glibenclamide administration on brain repair and its correlation with functional outcomes after stroke.

Our previous studies also showed that reactive microglia increase their expression of the K_{ATP}-channel components Kir6.1, Kir6.2, SUR1 and SUR2B after brain pathologies, and the *in vitro* pharmacology of the K_{ATP}-channel open state regulates the release of cytokines/chemokines.[8,11,12] More precisely, glibenclamide increased the reactive

morphology, phagocytic capacity and TNF-α secretion of reactive microglia *in vitro*. Thus, as cerebral ischemia leads to an accumulation of microglia in the subventricular zone (SVZ), from where newly formed neuroblasts migrate towards the ischemic boundary zone,[13] is likely that controlling the phenotype of activated microglia will promote brain repair. This will provide neuroprotection[14] and pro-neurogenic mediators that support the different steps of neurogenesis.[15,16] Indeed, stroke induces cortical neurogenesis in animals models,[17,18] and more importantly, in the adult human brain.[19,20] Whether microglia influence these processes and the fate of the newborn neurons is still unclear. Nonetheless, although there is contradictory evidence for microglia being pro-neurogenic, several recent findings reinforce the hypothesis that microglia can direct neurogenesis.[16,21]

Thus, we hypothesized that early blockade of SUR1 by glibenclamide after cerebral ischemia enhances ischemia-induced neurogenesis in the striatum and long-term brain repair, thus leading to an improved functional outcome. To test this hypothesis we treated rats with low doses of glibenclamide i.v. early after focal cerebral ischemia and evaluated long-term neuroprotection, neurogenesis, angiogenesis and behavioral recovery. Next, to assess whether microglia could be involved in neurogenesis, we analyzed the expression *in vivo* of SUR1 by reactive microglia after ischemia and whether glibenclamide binds specifically to microglia using primary rat microglia cultures.

METHODS

Transient Occlusion of the Middle Cerebral Artery in Rats

Male Wistar rats (3 months old and weighing 250-300 g at the beginning of the study; National Laboratory Animal Centre, Kuopio, Finland) were used. They were kept on a 12 h/12 h day and night cycle and housed individually with free access to food and water (20±1°C). Animals were handled following European legislation (86/609/EEC) and all efforts were made to minimize the number used and animal suffering, in accordance with the ARRIVE guidelines. The Animal Ethics Committee (Hämeenlinna, Finland) approved the study.

Focal cerebral ischemia was induced by the intraluminal filament technique as described elsewhere.[8] Briefly, the rats were anesthetized with 5% halothane (in 70% N_2O/30% O_2) and a surgical depth of anesthesia was maintained throughout the operation with 0.5 to 1% halothane delivered though a nose mask. The right common carotid artery was exposed through a midline cervical incision under a surgical microscope and gently separated from the nerves. A heparinized nylon filament (diameter 0.25 mm, rounded tip) was inserted into the stump of the external common carotid artery and advanced into the internal carotid artery 1.8-2.1 cm until it blocked the blood flow into the middle cerebral artery. Corticostriatal damage was induced by an occlusion of the middle cerebral artery (MCAO) of 90 min and the blood flow was then restored by removing the filament. Sham-operated control rats underwent the same procedure except that the filament was not inserted. To balance the MCAO groups the neurological symptoms were assessed before drug administration using two tests: contralateral rotation/circling behavior and impaired contralateral forelimb/hindlimb response to proprioceptive stimulus (i.e., lack of limb withdrawal when hanging over the edge of a table). Animals with no behavioral impairment were excluded from the study.

Drug Treatment

We divided 34 rats into the following three groups: sham-operated rats (n=10), vehicle-treated MCAO rats (n=12) and glibenclamide-treated MCAO rats (n=12). Rats were placed in a restrainer for drug administration in the distal portion of the vein. Each rat received three injections of 0.2 ml of either 0.01 mol/L phosphate buffer saline (PBS; pH 7.4) or 0.2 μg glibenclamide into the tail vein 6, 12 and 24 h after reperfusion (total dose 0.6 μg). Glibenclamide was prepared in DMSO and diluted in 0.01 mol/L PBS to final concentration (DMSO final concentration <0.5%). In order to analyze cell proliferation we administered intraperitoneal injections of BrdU (50 mg/kg in PBS 50 mmol/L), with some modifications, as described elsewhere.[22] In summary, all rats received a single injection of BrdU daily from postoperative days 4 to 8. Infarct volumes were measured at the end of the study and unsuccessful transient MCAO animals were excluded from the study (n=2 from vehicle group).

Behavioral Outcome Measures

Limb-PlacingTest

The modified version of the limb-placing test[23] was performed before operation and on postoperative days 2, 4, 7, 10, 13, 16, 19, 22, 26 and 29. The animals were habituated for handling and testing before the induction of ischemia. The test included seven limb-placing tasks to assess the integration of forelimb and hindlimb responses to tactile and proprioceptive stimulation. Briefly, animals were placed on the edge of a table and their forelimbs and hindlimbs were pushed over the edge to measure ability to retrieve their limbs. Tasks were performed from the front and the side of the rat, with and without the help of whisker stimuli. In addition, forepaw retraction was evaluated when the rat was lifted in the air by the base of its tail, and finally forepaw resistance was noted when the rat was pushed

on the table surface. Both sides of the body were tested to assess forelimb and hindlimb function. An observer blind to the experimental groups performed the behavioral analysis. Scoring: 2 points, normal response; 1 point, delayed and/or incomplete response; 0 points, no response.

Forelimb Asymmetry Test

The cylinder test was used to assess imbalance between impaired and non-impaired forelimbs.[24] Briefly, the rats were placed in a Plexiglas cylinder (Ø 20 cm) for at least 4 min or until the rats were observed to rear a minimum of 20 times. Sessions were videotaped from below the cylinder and analyzed using a slow motion video recorder to determine the number of contacts by both forelimbs and by either impaired or non-impaired forelimbs. An observer blind to the experimental groups performed the behavioral analysis. The cylinder score for an impaired forelimb was calculated as: contralateral contacts/total contacts x 100 %.

Tapered/Ledged Beam-Walking Test

The sensorimotor function of hindlimbs was evaluated using a tapered/ledged beam.[25] The beam-walking apparatus consisted of a tapered beam with underhanging ledges on each side to permit foot faults without falling and the end of the beam was connected to a black box. Steps onto the ledge were scored as a full slip and a half-slip was scored when the limb touched the side of the beam. The mean of three trials was used for statistical analyses. An observer blind to the experimental groups performed the behavioral analysis. Pretrained animals were tested in baseline conditions and on postoperative days 7 and 29. Performance was videotaped and analyzed by calculating the slip ratio (number of slips/number of total steps) of the impaired (contralateral to lesion) hindlimbs.

Morris Water-Maze

Spatial learning was assessed using a modified version of the Morris water-maze task.[23] Rats were given four trials per day on postoperative days 26 to 28 followed by the probe trial without the platform. The pool (Ø 150 cm) was divided into four quadrants or three annulus zones of equal surface area. Starting locations were called north, south, east, and west, and were located arbitrarily at equal distances along the pool rim. The platform was located in the middle of the northeast quadrant 25 cm from the pool rim. When the rat failed to find the hidden platform within 50 s, it was placed on the platform. The animal was allowed to remain on the platform for 10 s and to rest for 1 min after trials. The starting point was changed after each trial. The swim paths were monitored by a video camera connected to a computer through an image analyzer (HVS image). Escape latency (time to reach the platform) and the path length the animal swam to find the platform were parameters used to assess their performance in the water-maze task. Swimming speed (path length/escape latency) was calculated to exclude the effect of sensorimotor impairment. At the end of the third testing day, a 30 s probe trial without the platform was used to evaluate how well rats remembered the location of the platform (passes over the previous platform location). An observer blind to the experimental groups performed the behavioral analysis. Time spent in different annulus zones and quadrants of the pool was analyzed to examine the search strategies used by the animals.

Immunohistochemistry

Thirty days after MCAO, rats were anesthetized and transcardially perfused with saline for 5 min, followed by 4% w/v paraformaldehyde in phosphate buffer. Brains were post-fixed, cryopreserved in 30% w/v sucrose and frozen on dry ice. Sections (14 μm) covering the entire brain were cut with a cryotome.

The first section between bregma +1.7 and +2.2 of each animal stained with standard Haematoxylin-Eosin (H&E) was selected at random. Sequential sections separated by 1 mm were selected for each animal to determine the total infarct volume using the optical microscope software AxioVision 4 AC (Zeiss) and applying the Cavalieri's principle. This consisted of multiplying the infarct area by the distance between sections (1 mm) and combining the values from each section (5-6 sections/animal). The total infarct volume was calculated by subtracting the area of the remaining tissue in the ischemic hemisphere from the area of the intact contralateral tissue of each section.[23]

Immunohistochemistry was carried out with the avidin-biotin peroxidase method as previously described.[8] We used primary antibodies against doublecortin (DCX; clone C-18; 1:150; Santa Cruz) to detect undifferentiated neurons and NeuN (1:150; Chemicon), calbindin (CB; 1:500; Swant), parvalbumin (PV; 1:2000; Swant), tyrosine hydroxylase (TH; 1:5000; AbCam) or calretinin (CR; 1:2000; Swant) for differentiated neurons.[26] To detect blood vessels we used RECA-1 (1:100; Serotec). For glial detection, we used antibodies against GFAP (1:400; Sigma-Aldrich), CD11b (OX-42 clone; 1:150; Serotec) or the isolectin B4 peroxidase-conjugated (IB4) from *Bandeiraea simplicifolia* (1:25; Sigma-Aldrich). We used an antibody against the sulfonylurea receptor 1 (SUR1; 1:100, Santa Cruz) to detect the glibenclamide target in microglial cells. The fate of the new proliferating cells was determined by double immunostaining with mouse monoclonal anti-BrdU antibody (1:100; Sigma-Aldrich) and biotin-conjugated rat anti-mouse IgG (1:150) and antibodies against specific cellular markers, as described elsewhere.[26] ExtrAvidin-FITC (1:250; Sigma-Adrich) was used to detect BrdU-positive cells. Also, for immunofluorescence we used primary antibodies against NeuN (1:150; Chemicon), GFAP (1:400; Sigma-Aldrich), CD11b (OX-42 clone; 1:150; Serotec) and caspase-3 (clone 5A1E; 1:500; Cell Signalling). Then we used specific anti-IgGs conjugated with AlexaFluo-488 (1:300; Invitrogen) to detect caspase-3 and

specific anti-IgGs from various species conjugated with AlexaFluo-555 (1:300; Invitrogen) for the other cellular markers. Confocal images were acquired using a Leica TCS SL laser scanning confocal spectral microscope (Leica Microsystems Heidelberg GmbH, Mannheim, Germany) and images were analyzed with ImageJ 1.39u (NIH, USA).

Degenerating neurons were detected by Fluorojade B (FJB, Chemicon) fluorochrome, following the manufacturer's instructions.

Stereological methods were used to quantify the number of cells in the peri-infarct areas as described elsewhere.[8] We applied the optical fractionator method to count labeled cells. Peri-infarct regions were outlined at cortical and subcortical levels at 2.5x magnification on arbitrary uniform random (AUR) coronal sections, located throughout the entire brain. Individual cells were viewed at 40x in AUR-sampled sites chosen by the Mercator Pro 7.0 software (ExploraNova) and then counted.

Cell Culture and Microglial Activation

Cell culture procedures were approved by the Ethics Committee of the *Universitat de Barcelona*, in accordance with the regulations established by the Catalan autonomous government (*Generalitat de Catalunya*). Primary microglia-enriched cultures were obtained from post-natal-day-one rat brains, following the protocol described by Saura and colleagues [27], with slight modifications. Briefly, mixed glial cultures from post-natal-day-one rat brains were obtained from cerebral cortex and digested with 0.25% trypsin-EDTA solution (Invitrogen) for 30 min at 37ºC. Trypsinization was stopped by adding an equal volume of culture medium, consisted in Dulbecco's modified Eagle medium-F-12 nutrient mixture (DMEM:F12, Invitrogen) supplemented with 10% FBS, 0.1% penicillin-streptomycin (Invitrogen), 0.5 µg/mL amphotericin B (Fungizone®, Invitrogen), and 0.04% deoxyribonuclease I (Sigma-Aldrich). Cells were pelleted (8 min, 1000 rpm), resuspended in

culture medium, and brought to a single cell suspension by pipetting vigorously and filtering through a 105 µm-pore mesh. Cells suspension were seeded at a density of $3 \cdot 10^5$ cells/mL and grown in a humidifier cell incubator containing 5% CO_2 at 37ºC. Medium was replaced every 7 days. Microglial cultures were prepared by the mild trypsinization method after 19–21 days in vitro (DIV), where mixed glial cultures were treated for 30 min with 0.06% trypsin-EDTA solution. That resulted in a 97%-enriched microglial culture.

These microglial cultures were activated and treated 24 h after isolation as described below. Based on our preliminary results, cell cultures were pre-treated with 1 nmol/L glibenclamide diluted in culture medium (DMSO final concentration <0.05%; Sigma-Aldrich, >99% purity).[8] Thirty minutes later, cells were activated with 0.1 µg/mL of recombinant lipopolysaccharide (LPS) and 0.05 ng/mL of recombinant mouse interferon gamma (IFNγ; Sigma-Aldrich). After 48 h, cells were incubated for 30 min at 37ºC in HBSS and supplemented with 500 nmol/L glibenclamide–BODIPY-FL (green fluorescent dye; Invitrogen). After cell fixation with 4% w/v paraformaldehyde, we performed immunocytochemical analyses with mouse anti-rat CD11b (OX-42 clone; 1:500; Serotec) antibody and goat anti-mouse AlexaFluor-555 as a secondary antibody (1:500; Molecular Probes). Cultures were directly observed in an AxioObserver Z1 (Carl Zeiss; GmbH, Germany) inverted microscope equipped with FluoUp and CoLoc image software (ExploraNova, La Rochelle, France) and recorded on a high sensitivity camera (RetigaEXi Fast 1394, QImaging). Image processing was performed using the method described by Jaskolski and colleagues.[28] The purity of the cultures was 97±1% (n=4 cultures), as based on the number of CD11b-positive compared to the total number of cell nuclei stained with Hoescht33258 (Invitrogen; 0.1 µg/ml in PBS).

Statistical Analyses

Statgraphics 5.0 (STSC Inc., Rockville, MD) and GraphPad Prism4 (La Jolla, CA, USA) statistical packages were used. *In vitro* and histological data and differences in the infarct volumes between vehicle controls and glibenclamide-treated MCAO rats were analyzed using ANOVA followed by post hoc test Least Significant Difference (LSD). When normality was not reached, we applied the Kruskall-Wallis test followed by the Mann-Whitney *U*-test. Differences in the limb-placing scores between experimental groups were analyzed by the Mann-Whitney U-test. We used repeated measures ANOVA to analyze the beam-walking, cylinder and water-maze data for the overall group effect. Groups were then compared using one-way ANOVA followed by a post hoc test LSD. Probe trial data were tested by ANOVA followed by LSD. All values are presented as mean ± standard error of mean (SEM). P values <0.05 were considered significant.

RESULTS

Infarct Size, Gliosis, Neurodegeneration and Apoptosis

We analyzed the effects of glibenclamide in terms of lesion volume by histological methods 30 days after MCAO. Quantification of the lesion volume of Hematoxilin-Eosin stained sections showed that there was no difference in infarct volume size between vehicle- and glibenclamide-treated MCAO rats (Figure 1 A). We then performed stereological quantification of the MCAO-induced neuronal loss in the peri-infarcted volume by NeuN immunohistochemistry. Stereological counting showed same number of NeuN-positive cells in the peri-infarct striatum (Figure 1 B), but higher number in the peri-infarct cortex of glibenclamide-treated MCAO rats (Figure 1 C, $P<0.05$).

The pattern and cell density of microglia/macrophages (IB4-stained) and astrocytes (GFAP-immunopositive) in ischemic animals showed activation, as evidenced by their reactive morphology (Supplemental figure 1 C). In addition, when we quantified the overall staining and cell density for both markers, we found that glibenclamide did not modify MCAO-induced astrogliosis or microgliosis in the cortex (Supplemental figure 1 A, B).

As hypoxia and ischemia causes neuronal death in the peri-infarcted region, and consequently, secondary neurodegeneration in other brain regions, we analyzed whether neurodegenerative processes were still active one month after MCAO by Fluoro-Jade B (FJB) staining. Only scattered FJB-positive neurons were detected in the thalamus (Supplemental figure 2 A). We also studied apoptosis using cleaved caspase-3 immunohistochemistry. Cleaved caspase-3 staining did not co-localize with neurons (NeuN) or astrocytes (GFAP) (Supplemental figure 2 B, C). However, cleaved caspase-3 staining co-localized with some cells expressing the microglial/macrophage marker CD11b in the peri-infarct region (Supplemental figure 2 D). These results suggest that, one month after ischemia secondary neurodegenerative processes had completed.

Characterization of neuroblast migration and long-term neurogenesis

We hypothesized that glibenclamide treatment could influence neurogenesis after stroke. Firstly, DCX-immunohistochemistry was carried out to detect neuroblasts in the striatum migrating towards the lesion core to a group of rats sacrificed three days after MCAO (Sham n=3; MCAO groups n=6). Results showed that sham-operated animals had all DCX-positive cells attached to the intact lateral striatum or migrating through the rostral migratory stream (RMS). Contrary, MCAO animals showed increased migration of neural progenitor cells toward the infarct striatum (Figure 2 A, B) as reported previously.[13,22] Interestingly, we found more migrating neuroblasts in the striatum of glibenclamide-treated than in vehicle-treated MCAO rats ($P<0.001$, Figure 2 A, B). Neuroblast migration towards the infarct core in the striatum was still active 30 days after MCAO (Figure 2 C, D) and the migration pattern was not altered by glibenclamide administration. In line, microglia from the striatum adjacent to the ventricle became reactive after ischemia, but we did not observe a change in their morphology driven by glibenclamide treatment (Figure 2 A).

Secondly, to detect cell proliferation we sacrificed a group of rats 30 days after MCAO (sham n=9; vehicle n=10 and glibenclamide-treated group n=12). Immunohistochemistry against BrdU showed that vehicle-treated MCAO rats had more BrdU-positive cells in the cerebral cortex ($P<0.001$) than sham-operated rats (Figure 3 A). Glibenclamide treatment increased the number of BrdU-positive cells in the cerebral cortex ($P<0.001$) and in the CA1 pyramidal layer ($P<0.05$; glibenclamide vs. sham) (Figure 3 A). Then, using the same group of animals, we performed double immunohistochemistries to identify the cell lineage of proliferative cells (Figure 3 A, B). Quantitative results showed an increased number BrdU/NeuN-positive cells in the cerebral cortex in vehicle-treated MCAO rats ($P<0.001$) and this was further boosted by glibenclamide treatment ($P<0.001$; glibenclamide vs. vehicle-

treated MCAO rats). A slight increase in the number of BrdU/NeuN-positive cells was found in the CA1 region and in the SGZ of the hippocampus, although this increase was not statistically significant compared to the vehicle group ($P<0.05$; glibenclamide vs. sham). In addition, the other neuronal population markers (e.g., parvalbumin, tyrosine hydroxylase, calbindin) were also analyzed, but did not co-localize with BrdU (data not shown). The number of BrdU/GFAP-positive cells increased in the cortex of vehicle-treated MCAO rats ($P<0.001$) (Figure 3 A, B), pointing to an astroglial proliferation caused by the lesion. Also in the cortex glibenclamide-treated MCAO rats showed increased astroglial proliferation ($P<0.001$) compared to sham-operated rats and vehicle-treated MCAO rats. We then analyzed macrophages/microglia proliferation, and we observed an increased number of BrdU/IB4-stained cells in the cortex ($P<0.001$) and in the CA1 pyramidal layer ($P<0.001$) of MCAO rats (Figure 3 A, B).

To study whether glibenclamide modifies the fate of the neuroblasts as they migrate through the RMS, we quantified the number of BrdU-positive cells in the olfactory bulb 30 days after MCAO. No differences in the number of these cells were found between MCAO groups in the olfactory bulb (542±26 BrdU-positive cells/section for sham, 518±37 for vehicle-treated group and 580±28 for glibenclamide-treated group). As the total number of proliferative cells in the olfactory bulb is not modified by ischemia or glibenclamide, the most likely the fate of neuroblasts migrating through the RMS is also unaffected. Therefore, these results indicate that glibenclamide strengthens intrinsic neurogenic processes as higher numbers of NeuN/BrdU-positive cells were found in the cortex.

Angiogenesis

To assess another brain repair mechanism, we studied angiogenesis in several brain regions by measuring vessel diameter and RECA-1 immunoreactivity 30 days after ischemia.[29] The

diameter of vessels increased in the ipsilateral cortex of glibenclamide-treated MCAO rats (Figure 4 A, C). Quantitative analysis of RECA-1 immunoreactivity showed increased microvessel density in the ipsilateral hippocampus of glibenclamide-treated MCAO rats (Figure 4 B, C; $P<0.01$). This difference was not detected in the peri-infarct cortex, although a slight increase was found.

Recovery of Sensorimotor and Cognitive Functions

The effects of ischemia and glibenclamide treatment in the recovery of sensorimotor and cognitive functions were analyzed using a battery of behavioral tests during a 30 days follow-up period. Spontaneous forelimb use was analyzed by the cylinder test (Figure 5 A). ANOVA for repeated measures showed an overall group effect ($P<0.05$), but no significant group x time interaction, thereby indicating that forelimb use differed between groups. A *post hoc* analysis revealed that forelimb use between sham-operated and vehicle-treated MCAO rats was different ($P<0.05$), but not between sham-operated and glibenclamide-treated MCAO rats. Forelimb use in the MCAO groups was different from that in sham-operated rats on postoperative day 7 ($P<0.01$). Impaired forelimb use in MCAO rats treated with glibenclamide was recovered and these animals showed similar performance to that of sham-operated rats at the end of the follow-up period.

We then used the limb-placing test to further analyze recovery of the forelimb function. All ischemic animals presented initial severe impairment in the limb-placing test after MCAO, followed by spontaneous recovery during the 29-day follow-up (Figure 5 B). Limb-placing scores between sham-operated and MCAO rats were different in all post-operative time points ($P<0.01$). MCAO rats treated with glibenclamide showed an improved score compared to the vehicle group on postoperative days 22 to 29 ($P<0.05$; $P<0.01$).

The effect of glibenclamide on recovery of hindlimb function in MCAO rats was analyzed by tapered/ledged beam-walking. ANOVA for repeated measures showed an overall group effect ($P<0.01$) and a group x day interaction ($P<0.01$). However, there was no difference between glibenclamide-treated and vehicle-treated MCAO rats ($p=0.81$) (data not shown).

Results from the Morris water-maze on post-operative days 26 to 28 showed that escape latency, length and swimming speed did not differ between groups. No significant differences were observed in the number of passes over the removed platform or the time rats spent in the target quadrant (probe trial). However, a thigmotaxis behavior was observed in vehicle-treated MCAO rats, which they spent more time in the outermost zone (zone 3; $P<0.05$) and less time in the middle zone (zone 2; $P<0.01$) compared to sham-operated animals (Figure 5 C-D). The search strategy in glibenclamide-treated MCAO rats was similar to that of sham-operated animals.

Glibenclamide Binds to Reactive Microglia

To assess whether microglia express the K_{ATP}-channel components after ischemia, we performed double immunohistochemical labeling against SUR1 and Kir6.2 combined with the microglia/macrophage marker CD11b. Co-location of striatal CD11b-positive cells adjacent to the ventricle indicated that the reactive microglia of MCAO animals expressed the K_{ATP}-channel components SUR1 and Kir6.2 at 72 h after ischemia (Figure 6 A). To determine the specificity of binding to SUR1 expressed by microglia, we analyzed the binding of fluorescently tagged glibenclamide (glibenclamide BODIPY FL; green fluorescence) in primary rat microglial cultures. When microglial cells were in the resting state, glibenclamide labeling was localized to the perinuclear space (Figure 6 B). Forty-eight hours after LPS+IFNγ activation, glibenclamide-labeling was present in the plasmalemmal

membrane, denoting a translocation of SUR1 from its internal reservoir towards the cell surface.

DISCUSSION

Previous preclinical and clinical data suggest a neuroprotective role for glibenclamide after cerebral ischemia.[3,4] Here we showed that glibenclamide also enhanced early migration of neuroblasts towards the striatal lesion core and facilitated long-term brain repair in MCAO rats. Interestingly, this was associated with improved behavioral recovery.

After a stroke, massive necrotic or apoptotic processes are activated in the ischemic core, as well as in distal regions due to Wallerian neurodegeneration. In our model we only observed a few scattered FJB positive neurodegenerative cells, which were mainly located in the thalamus one month after ischemia. In addition, the only cells labeled by cleaved caspase-3 in the peri-infarct zone were some microglia/macrophages. Recent data demonstrated that cleaved caspase-3, a known mediator of apoptosis, regulates microglial activation by a non-apoptotic pathway.[30] Thus, we here found that one month after ischemia the majority of secondary neurodegenerative processes have been completed and caspase-3 positive microglia/macrophages may be participating in the tissue repair response to injury instead of undergoing apoptosis. Although glibenclamide did not reduce the size of the infarct, our results are in line with Simard et al,[10] confirming that some factor other than infarct volume here also determined the long-term functional recovery outcome. Interestingly, in the Morris water maze task we observed thigmotaxis behavior in vehicle-treated MCAO animals (i.e., swimming close to the walls of the tank), which was decreased after glibenclamide treatment. However, whether thigmotaxis is related to cognitive or noncognitive strategies, or hippocampus-derived increases in stress or anxiety, still remain open.[31,32] Thus, from our data we cannot rule out the possibility that glibenclamide, instead of improving cognitive outcome, ameliorates stress or anxiety caused by ischemia. It is noteworthy to mention here that our approach for glibenclamide administration is different to that used by Simard et al,[3,7,10] who administered an intraperitoneal loading dose of 10 µg/kg plus a subcutaneous

infusion dose of 200 ng/h using an osmotic mini-pump. We administered glibenclamide intravenously with a dose of 0.8 µg/kg beginning 6 hours after onset of ischemia during the first 24 hours. The facts that the subunit SUR1 has a particularly high affinity for glibenclamide,[33] the ischemic brain shows preferential uptake for glibenclamide[7,8] and that we here use intravenous glibenclamide administration instead of subcutaneous infusion, could explain our results. However, the dose of glibenclamide was lower than the doses used in previous studies.

Focal cerebral ischemia promotes neurogenesis in the SVZ and the SGZ of the dentate gyrus and induces neuroblast migration towards the striatal ischemic boundary.[13,22] Recent data have provided new evidence that the cerebral cortex also has the same capacity,[17] and more importantly, stroke-induced cortical neurogenesis has also been found in the adult human brain.[19,20] In the present study, ischemia increased neuroblast migration towards the lesion 3 days after ischemia/reperfusion and this event persisted for up to one month. Inhibition of SUR1 using glibenclamide led to a further increase in the number of migrating neuroblasts, thereby indicating that glibenclamide modifies the cell lineage choice or enhances progenitor cell proliferation and migration.

Proliferative cells detected by administration of BrdU from days 4 to 8 after ischemia/reperfusion showed increased co-expression of NeuN in the peri-infarct area of the cortex 30 days after reperfusion and this was potentiated by glibenclamide. Although we cannot exclude the possibility that some neural progenitors migrate from the SVZ to establish themselves in the ipsilateral cortical network, we found no co-localization of BrdU-positive cells with the classical RMS derived neuronal markers (i.e., calbindin, calretinin, tyrosine hydroxylase, parvalbumin) and no change in the total number of proliferative cells in the olfactory bulb. Thus, these newborn cortical neurons may have originated from potential resident neural stem cells within the cortex.[17] Several authors have proposed that these

endogenous quiescent neural stem cells are present in the cerebral cortex and that their proliferation and differentiation to mature neurons is induced by ischemic insults.[18] Although the number of these cells may be small, strategies to foster their intrinsic neurogenic potential would be highly relevant for clinical approaches to facilitate neural repair and functional recovery.

Another purpose of this study was to investigate angiogenesis after cerebral infarction, because angiogenesis is also activated after cerebral ischemia. Generally, tissue repair is activated at 2 to 3 days after reperfusion, and the infarction is eventually encircled by a glial scar a few weeks later. As the glial response, in terms of the reactive area or cell density, was not modified by glibenclamide, we analyzed the microvessel diameter and the surface density as a parameter to quantify angiogenesis.[29] We herein demonstrated that glibenclamide causes microvascular changes, where interestingly, glibenclamide further increased the diameter of microvessels in the non-lesioned cortex and RECA-1 immunoreactivity in the hippocampus, and both regions showed glial proliferation. These observations are consistent with those of Fantin and colleagues,[34] who reported that tissue macrophages/microglia are associated with angiogenesis in various developing organs. Vasculature attracts microglial cells and stimulates them to release angiogenic factors,[35] with subsequent growth stimulation of neural stem cells.[36] Furthermore, angiogenesis is considered a key feature of ischemic stroke recovery and neuronal post-stroke re-organization.[37]

Several studies using experimental stroke models have indicated the beneficial effects of glibenclamide administration after reperfusion, such as reversing ischemia-reperfusion injury by halting oxidative stress and inflammation in the hippocampus,[9] preventing cytotoxic edema after cerebral ischemia[2,3,1,7] and enhancing neuroprotection, which all eventually lead to a better functional outcome.[8] Thus, although glibenclamide did not modify the size and cell density of microglia nor astroglia after ischemia here, it enhanced long-term brain repair

processes and functional recovery outcomes of the rats. We recently reported that 72 h after MCAO, activated microglia/macrophages in the ischemic hemisphere increase K_{ATP}-channel expression, and so does the murine microglial BV2 cell line 48 h after inflammatory stimuli.[8] We have now confirmed these results in postnatal primary rat microglial cultures. When microglial cells became activated after pro-inflammatory stimuli, they showed higher specific glibenclamide-labeling and the signal extended to the plasmalemmal membrane *in vitro*, pointing towards a mobilization of SUR1 from its internal reservoir in the endoplasmic reticulum and Golgi apparatus, towards the cell surface. Also, reactive microglia located in the lateral striatum 72 hours after MCAO expressed the K_{ATP}-channel components SUR1 and Kir6.2. All these results suggest that after microglial activation, K_{ATP}-channel expression is increased and the channel becomes translocated to the cell surface where it can exert its function in brain pathologies. *In vitro* glibenclamide regulates microglial phagocytic activity and the release of cytokines/chemokines after pro-inflammatory stimuli.[8,11] As postnatal and adult microglia constitutively express low levels of SUR1,[8,11,12] it is likely that regardless of the age of the animal the expression of SUR1 is upregulated by cell death/damage signals. Nonetheless, although glibenclamide possibly also blocks the SUR1 subunits of K_{ATP}- or $NC_{Ca\text{-}ATP}$-channels expressed in neurons, astrocytes and capillary endothelial cells,[2,3] there is increasing evidence that microglia participate in modifications of stem cell proliferation, migration and/or differentiation by producing trophic factors and inflammatory cytokines/chemokines.[15,16] Thus, as microglial activation is a dynamic and complex process,[38] the pro- or anti-neurogenic niche would depend on the degree of microglial activation and the balance between the pro- and anti-inflammatory soluble cytokines produced, without cell-cell contact required to direct this effect.[16,21] In this scenario, it is possible that the interaction of glibenclamide with SUR1 endows microglia from the lateral striatum to carry a distinct phenotype that releases soluble factors with paracrine effects,

which consequently enhance neurogenesis and the migration of neuroblasts towards the lesion.

In summary, we have demonstrated here that early blockade of SUR1 by glibenclamide produces long-term cortical neuroprotection, stimulates neuroblast migration towards the striatal lesion and strengthens neurogenesis in the cortex after cerebral ischemia. All these results were temporally associated with improved long-term behavioral recovery. Therefore, these data identify SUR1 as a multifaceted target that promotes both long-term neuroprotective processes and brain repair mechanisms. Further experiments are necessary to identify the specific role of the microglial K_{ATP}-channel and its diffusible mediators that may modulate brain repair, which will help us to shed light on the understanding of the intricate mechanisms underlying neurogenesis and neuroprotection after stroke caused by glibenclamide treatment.

Disclosures

NM and MJR hold an EU patent (No. WO2006/000608). The other authors report no disclosures.

Supplementary information is available at the Journal of Cerebral Blood Flow and Metabolism website – http://www.nature.com/jcbfm

References

1. Simard JM, Woo SK, Schwartzbauer GT, Gerzanich V. Sulfonylurea receptor 1 in central nervous system injury: A focused review. *J Cereb Blood Flow Metab*. 2012
2. Simard JM, Tsymbalyuk N, Tsymbalyuk O, Ivanova S, Yurovsky V, Gerzanich V. Glibenclamide is superior to decompressive craniectomy in a rat model of malignant stroke. *Stroke*. 2010;41:531-537
3. Simard JM, Yurovsky V, Tsymbalyuk N, Melnichenko L, Ivanova S, Gerzanich V. Protective effect of delayed treatment with low-dose glibenclamide in three models of ischemic stroke. *Stroke*. 2009;40:604-609
4. Kunte H, Schmidt S, Eliasziw M, del Zoppo GJ, Simard JM, Masuhr F*, et al.* Sulfonylureas improve outcome in patients with type 2 diabetes and acute ischemic stroke. *Stroke*. 2007;38:2526-2530
5. Mikhailov MV, Campbell JD, De Wet H, Shimomura K, Zadek B, Collins RF*, et al.* 3-K structural and functional characterization of the purified K_{ATP} channel complex Kir6.2-SUR1. *EMBO J*. 2005;24:4166-4175
6. Chen M, Simard JM. Cell swelling and a nonselective cation channel regulated by internal Ca^{2+} and ATP in native reactive astrocytes from adult rat brain. *J Neurosci*. 2001;21:6512-6521
7. Simard JM, Chen M, Tarasov KV, Bhatta S, Ivanova S, Melnitchenko L*, et al.* Newly expressed SUR1-regulated $NC_{Ca\text{-}ATP}$ channel mediates cerebral edema after ischemic stroke. *Nat Med*. 2006;12:433-440
8. Ortega FJ, Gimeno-Bayon J, Espinosa-Parrilla JF, Carrasco JL, Batlle M, Pugliese M*, et al.* ATP-dependent potassium channel blockade strengthens microglial neuroprotection after hypoxia-ischemia in rats. *Exp Neurol*. 2012;235:282-296

9. Abdallah DM, Nassar NN, Abd-El-Salam RM. Glibenclamide ameliorates ischemia-reperfusion injury via modulating oxidative stress and inflammatory mediators in the rat hippocampus. *Brain Res*. 2011;1385:257-262

10. Simard JM, Woo SK, Tsymbalyuk N, Voloshyn O, Yurovsky V, Ivanova S*, et al.* Glibenclamide-10-h treatment window in a clinically relevant model of stroke. *Transl Stroke Res*. 2012;3:286-295

11. Virgili N, Espinosa-Parrilla JF, Mancera P, Pastén-Zamorano A, Gimeno-Bayon J, Rodríguez MJ*, et al.* Oral administration of the K_{ATP} channel opener diazoxide ameliorates disease progression in a murine model of multiple sclerosis. *J Neuroinflammation*. 2011;8:149

12. Ramonet D, Rodriguez MJ, Pugliese M, Mahy N. Putative glucosensing property in rat and human activated microglia. *Neurobiol Dis*. 2004;17:1-9

13. Thored P, Heldmann U, Gomes-Leal W, Gisler R, Darsalia V, Taneera J*, et al.* Long-term accumulation of microglia with proneurogenic phenotype concomitant with persistent neurogenesis in adult subventricular zone after stroke. *Glia*. 2009;57:835-849

14. Carson MJ, Doose JM, Melchior B, Schmid CD, Ploix CC. CNS immune privilege: Hiding in plain sight. *Immunol Rev*. 2006;213:48-65

15. Ekdahl CT, Kokaia Z, Lindvall O. Brain inflammation and adult neurogenesis: The dual role of microglia. *Neuroscience*. 2009;158:1021-1029

16. Butovsky O, Ziv Y, Schwartz A, Landa G, Talpalar AE, Pluchino S*, et al.* Microglia activated by IL-4 or IFN-gamma differentially induce neurogenesis and oligodendrogenesis from adult stem/progenitor cells. *Mol Cell Neurosci*. 2006;31:149-160

17. Shimada IS, Peterson BM, Spees JL. Isolation of locally derived stem/progenitor cells from the peri-infarct area that do not migrate from the lateral ventricle after cortical stroke. *Stroke*. 2010;41:e552-e560

18. Jiang W, Gu W, Brannstrom T, Rosqvist R, Wester P. Cortical neurogenesis in adult rats after transient middle cerebral artery occlusion. *Stroke*. 2001;32:1201-1207

19. Macas J, Nern C, Plate KH, Momma S. Increased generation of neuronal progenitors after ischemic injury in the aged adult human forebrain. *J Neurosci*. 2006;26:13114-13119

20. Jin K, Wang X, Xie L, Mao XO, Zhu W, Wang Y*, et al.* Evidence for stroke-induced neurogenesis in the human brain. *Proc Natl Acad Sci USA*. 2006;103:13198-13202

21. Walton NM, Sutter BM, Laywell ED, Levkoff LH, Kearns SM, Marshall GP*, et al.* Microglia instruct subventricular zone neurogenesis. *Glia*. 2006;54:815-825

22. Arvidsson A, Collin T, Kirik D, Kokaia Z, Lindvall O. Neuronal replacement from endogenous precursors in the adult brain after stroke. *Nat Med*. 2002;8:963-970

23. Puurunen K, Jolkkonen J, Sirviö J, Haapalinna A, Sivenius J. An alpha(2)-adrenergic antagonist, atipamezole, facilitates behavioral recovery after focal cerebral ischemia in rats. *Neuropharmacology*. 2001;40:597-606

24. Karhunen H, Pitkänen A, Virtanen T, Gureviciene I, Pussinen R, Ylinen A*, et al.* Long-term functional consequences of transient occlusion of the middle cerebral artery in rats: A 1-year follow-up of the development of epileptogenesis and memory impairment in relation to sensorimotor deficits. *Epilepsy Res*. 2003;54:1-10

25. Zhao C-S, Puurunen K, Schallert T, Sivenius J, Jolkkonen J. Effect of cholinergic medication, before and after focal photothrombotic ischemic cortical injury, on histological and functional outcome in aged and young adult rats. *Behav Brain Res*. 2005;156:85-94

26. Valente T, Hidalgo J, Bolea I, Ramirez B, Anglés N, Reguant J*, et al.* A diet enriched in polyphenols and polyunsaturated fatty acids, LMN diet, induces neurogenesis in the subventricular zone and hippocampus of adult mouse brain. *J Alzheimers Dis*. 2009;18:849-865

27. Saura J, Tusell JM, Serratosa J. High-yield isolation of murine microglia by mild trypsinization. *Glia*. 2003;44:183-189

28. Jaskolski F, Mulle C, Manzoni OJ. An automated method to quantify and visualize colocalized fluorescent signals. *J Neurosci Methods*. 2005;146:42-49

29. Czéh B, Abumaria N, Rygula R, Fuchs E. Quantitative changes in hippocampal microvasculature of chronically stressed rats: No effect of fluoxetine treatment. *Hippocampus*. 2010;20:174-185

30. Burguillos MA, Deierborg T, Kavanagh E, Persson A, Hajji N, Garcia-Quintanilla A*, et al.* Caspase signalling controls microglia activation and neurotoxicity. *Nature*. 2011:1-7

31. Goss CW, Hoffman SW, Stein DG. Behavioral effects and anatomic correlates after brain injury: A progesterone dose-response study. *Pharmacol Biochem Behav*. 2003;76:231-242

32. Mendez IA, Montgomery KS, LaSarge CL, Simon NW, Bizon JL, Setlow B. Long-term effects of prior cocaine exposure on morris water maze performance. *Neurobiol Learn Mem*. 2008;89:185-191

33. Dörschner H, Brekardin E, Uhde I, Schwanstecher C, Schwanstecher M. Stoichiometry of sulfonylurea-induced ATP-sensitive potassium channel closure. *Mol Pharmacol*. 1999;55:1060-1066

34. Fantin A, Vieira JM, Gestri G, Denti L, Schwarz Q, Prykhozhij S*, et al.* Tissue macrophages act as cellular chaperones for vascular anastomosis downstream of VEGF-mediated endothelial tip cell induction. *Blood*. 2010;116:829-840

35. Rymo SF, Gerhardt H, Wolfhagen Sand F, Lang R, Uv A, Betsholtz C. A two-way communication between microglial cells and angiogenic sprouts regulates angiogenesis in aortic ring cultures. *PLoS ONE*. 2011;6:e15846

36. Androutsellis-Theotokis A, Rueger MA, Park DM, Boyd JD, Padmanabhan R, Campanati L*, et al.* Angiogenic factors stimulate growth of adult neural stem cells. *PLoS ONE*. 2010;5:e9414

37. Slevin M, Kumar P, Gaffney J, Kumar S, Krupinski J. Can angiogenesis be exploited to improve stroke outcome? Mechanisms and therapeutic potential. *Clin Sci*. 2006;111:171-183

38. Schwartz M, Butovsky O, BrÅck W, Hanisch UK. Microglial phenotype: Is the commitment reversible? *Trends in Neuroscience*. 2006;29 68-74

Titles and Legends to Figures

Figure 1. Glibenclamide does not affect corticostriatal infarct size in MCAO rats (**A**). Quantification of NeuN-positive cells in the peri-infarct striatum **(B)** and cortex **(C).** Results are mean±SEM (n=10-12). **P*<0.05 (compared with vehicle-treated MCAO rats).

Figure 2. Glibenclamide enhances neuroblast migration towards the ischemic lesion. Representative micrographs of doublecortin (DCX) and microglia/macrophage (IB4) immunostaining in the striatum adjacent to the ventricle of sham-operated rat and vehicle- and glibenclamide- (Gbc, 0.6µg) treated MCAO rats three days after ischemia (**A**). Quantitative analysis of the migrating neuroblasts/section toward the cadoputamen lesion (**B**). Coronal section representation of an ischemic rat brain (bregma -0.8), where dark pink denotes for the necrotic core, light pink for peri-infarct area and green for healthy tissue (**C**). Enlarged image of the blue box from the left, in which DCX-positive cells (red) were still present in the peri-infarct striatum 30 days after MCAO (asterisk denotes the striatal lesion core) (**D**). Results are mean±SEM (n=3-6). ****P*<0.001 (compared with sham rats); $^{\#\#\#}P$<0.001 (compared with vehicle-treated MCAO rats). Bar=50 µm.

Figure 3. Characterization of proliferative cells into the ischemic brain. Quantitative analysis of the total number of BrdU-positive cells/section and relative number of neurons (NeuN), astrocytes (GFAP) and microglia (IB4) double stained BrdU-positive cells in the cortex, CA1 pyramidal cell layer and subgranular zone (SGZ) (**A**). Confocal photomicrographs of the rat cortex showing colocalization of BrdU (in green) with NeuN, GFAP and IB4 (red) (**B**). Glibenclamide increased the total number of BrdU-positive cells after MCAO. These cells preferentially co-localized with markers of neurons and astrocytes.

Bar 10 μm. Results are mean±SEM (n=9-10). *P<0.05 (total BrdU-positive cells compared with sham rats); $^{\#}P$<0.05 (total BrdU-positive cells compared with vehicle-treated MCAO rats); ^{++}P<0.01,^{+++}P<0.001 (cell type compared with sham rats); $^{\&\&}P$<0.01, $^{\&\&\&}P$<0.001 (cell type compared with vehicle-treated MCAO rats).

Figure 4. Glibenclamide foster angiogenesis in the cortex and hippocampus of ischemic animals. Quantitative analysis of the microvessel diameter (**A**) and RECA-1 immunoreactivity (**B**) in the cortex and hippocampus after MCAO. Glibenclamide administration increased microvessel diameter in the non-lesioned cortex and RECA-1 immunoreactivity in the hippocampus. Representative micrographs of RECA-1 immunoreactive microvessels in the cortex of sham-operated rat, vehicle- and glibenclamide-treated (0.6μg) MCAO rats (**C**). Bar 50 μm. Results are mean±SEM (n=6-11). **P<0.01 (compared to sham and vehicle-treated MCAO rats).

Figure 5. Ischemic animals showed long-term improvement of neurological function after glibenclamide treatment. Contralateral forelimb use (cylinder test) (**A**) and limb-placing scores (**B**) during a 29-day follow-up after MCAO. Swimming strategy in the probe trial test (Morris water-maze) on postoperative day 28 (**C, D**). Here the values are shown as a percentage of time spent in equal zones of the pool. Zone 1 refers to the inner annulus and zone 3 the outermost annulus. Results are mean±SEM (n=9-12). *P<0.05; **P<0.01 (compared with sham-operated rats); $^{\#}P$<0.05; $^{\#\#}P$<0.01 (compared with vehicle-treated MCAO rats).

Figure 6. Reactive microglia express and translocate SUR1 to the cell surface. (**A**) Confocal photomicrographs of SUR1 and Kir6.2 (green) in reactive microglia ($CD11b^{+}$; red)

localized to the striatum adjacent to the ventricle in MCAO rats. Yellow in the merge image denotes colocalization, whereby reactive CD11b-postive cells expressed SUR1 or Kir6.2 seventy-two hours after ischemia. (**B**) Localization of glibenclamide (glibenclamide BODIPY FL; green fluorescence) in rat microglial primary culture. Non-activated or cultures activated with LPS+IFNγ for 48 h are shown in the upper row. Microglial cells were labeled with an anti-CD11b (red) antibody and Hoechst (blue) to stain the nuclei. Lower row shows respective colocalization of the red and green channels, where the yellow denotes the presence of the glibenclamide binding in microglial cells. Arrowhead denotes peri-nuclear colocalization and arrows show surface labeling; the data shown are representative of 4 experiments each. Scale bar in (A) is 15 μm and in (B) is 20 μm**.**

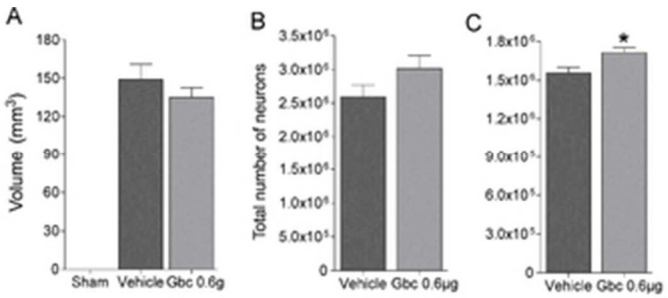

Figure 1. Glibenclamide does not affect corticostriatal infarct size in MCAO rats (A). Quantification of NeuN-positive cells in the peri-infarct striatum (B) and cortex (C). Results are mean±SEM (n=10-12). *P<0.05 (compared with vehicle-treated MCAO rats).
28x12mm (300 x 300 DPI)

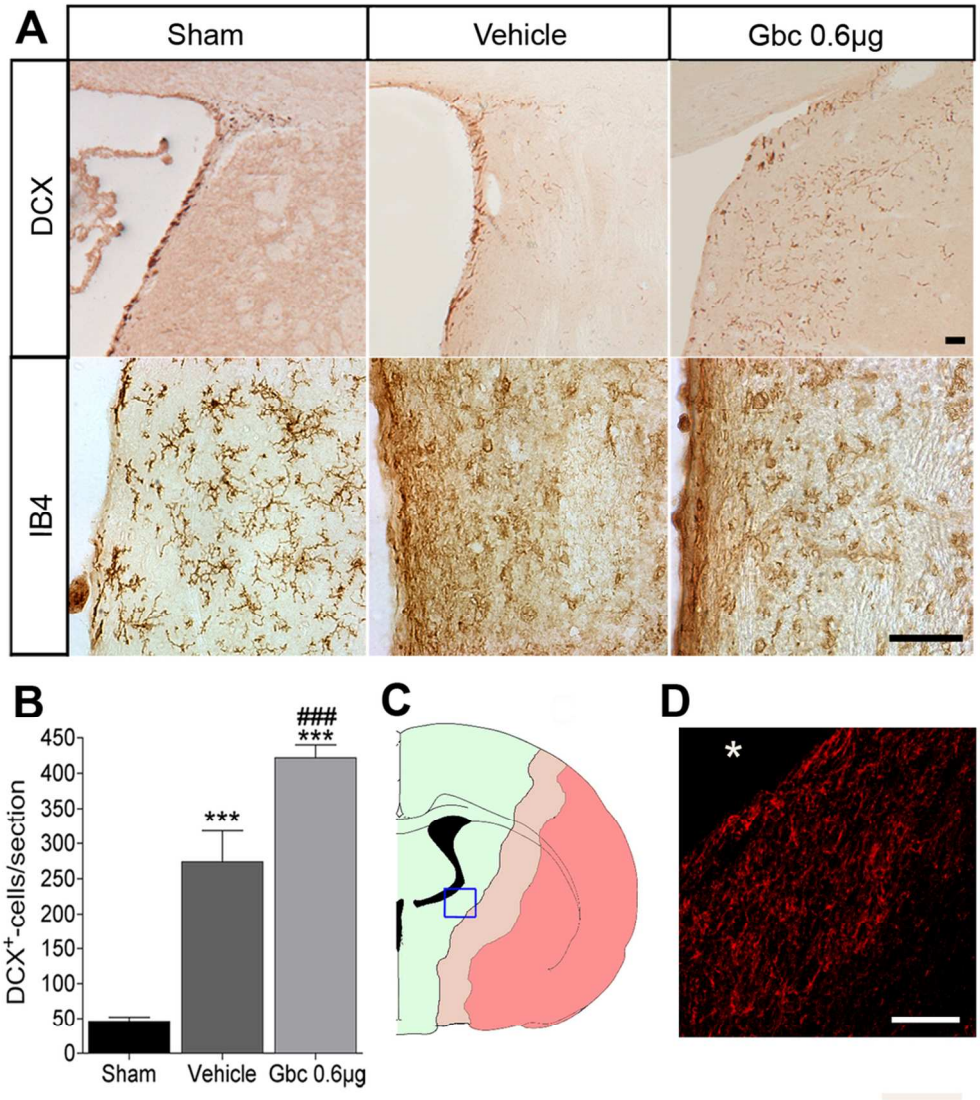

Figure 2. Glibenclamide enhances neuroblast migration towards the ischemic lesion. Representative micrographs of doublecortin (DCX) and microglia/macrophage (IB4) immunostaining in the SVZ of sham-operated rat and vehicle- and glibenclamide- (Gbc, 0.6µg) treated MCAO rats three days after ischemia (A). Quantitative analysis of the migrating neuroblasts/section toward the cadoputamen lesion (B). Coronal section representation of an ischemic rat brain (bregma -0.8), where dark pink denotes for the necrotic core, light pink for peri-infarct area and green for healthy tissue (C). Enlarged image of the blue box from the left, in which DCX-positive cells (red) were still present in the peri-infarct striatum 30 days after MCAO (asterisk denotes the striatal lesion core) (D). Results are mean±SEM (n=3-6). ***P<0.001 (compared with sham rats); ###P<0.001 (compared with vehicle-treated MCAO rats). Bar=50 µm.
97x109mm (300 x 300 DPI)

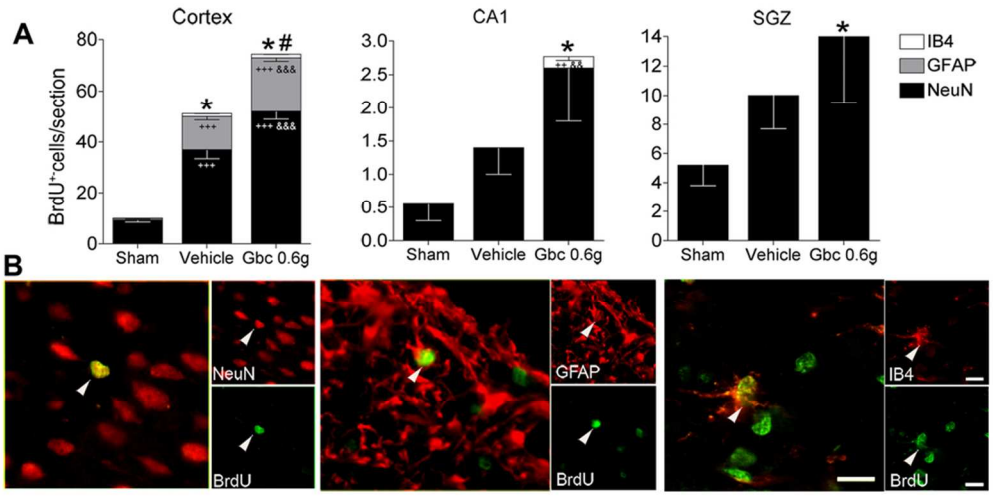

Figure 3. Characterization of proliferative cells into the ischemic brain. Quantitative analysis of the total number of BrdU-positive cells/section and relative number of neurons (NeuN), astrocytes (GFAP) and microglia (IB4) double stained BrdU-positive cells in the cortex, CA1 pyramidal cell layer and subgranular zone (SGZ) (A). Confocal photomicrographs of the rat cortex showing colocalization of BrdU (in green) with NeuN, GFAP and IB4 (red) (B). Glibenclamide increased the total number of BrdU-positive cells after MCAO. These cells preferentially co-localized with markers of neurons and astrocytes. Bar 10 μm. Results are mean±SEM (n=9-10). *P<0.05 (total BrdU-positive cells compared with sham rats); #P<0.05 (total BrdU-positive cells compared with vehicle-treated MCAO rats); ++P<0.01,+++P<0.001 (cell type compared with sham rats); &&P<0.01, &&&P<0.001 (cell type compared with vehicle-treated MCAO rats).
88x44mm (300 x 300 DPI)

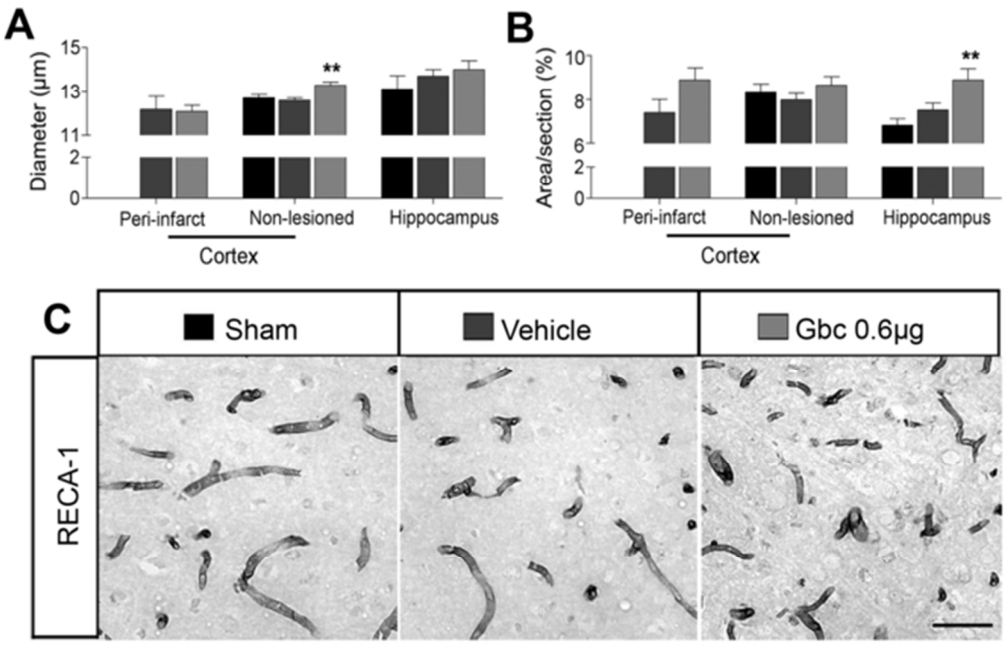

Figure 4. Glibenclamide foster angiogenesis in the cortex and hippocampus of ischemic animals. Quantitative analysis of the microvessel diameter (A) and RECA-1 immunoreactivity (B) in the cortex and hippocampus after MCAO. Glibenclamide administration increased microvessel diameter in the non-lesioned cortex and RECA-1 immunoreactivity in the hippocampus. Representative micrographs of RECA-1 immunoreactive microvessels in the cortex of sham-operated rat, vehicle- and glibenclamide-treated (0.6µg) MCAO rats (C). Bar 50 µm. Results are mean ± SEM (n=6-11). **P<0.01 (compared to sham and vehicle-treated MCAO rats).
55x36mm (300 x 300 DPI)

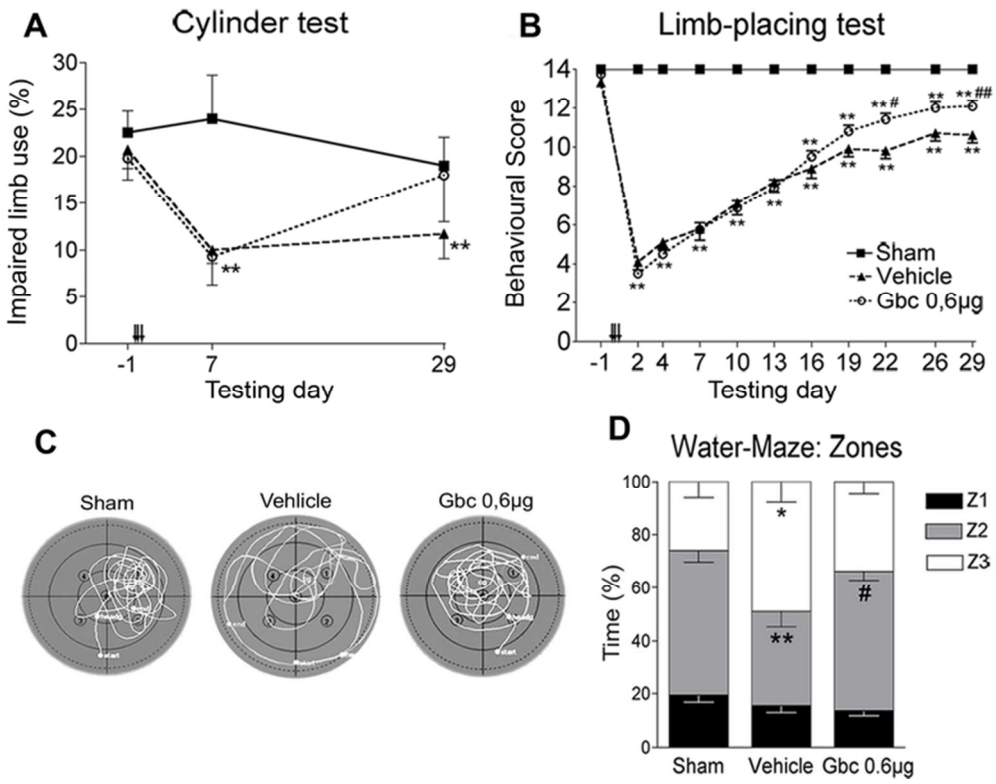

Figure 5. Ischemic animals showed long-term improvement of neurological function after glibenclamide treatment. Contralateral forelimb use (cylinder test) (A) and limb-placing scores (B) during a 29-day follow-up after MCAO. Swimming strategy in the probe trial test (Morris water-maze) on postoperative day 28 (C, D). Here the values are shown as a percentage of time spent in equal zones of the pool. Zone 1 refers to the inner annulus and zone 3 the outermost annulus. Results are mean±SEM (n=9-12). *P<0.05; **P<0.01 (compared with sham-operated rats); #P<0.05; ##P<0.01 (compared with vehicle-treated MCAO rats).
66x51mm (300 x 300 DPI)

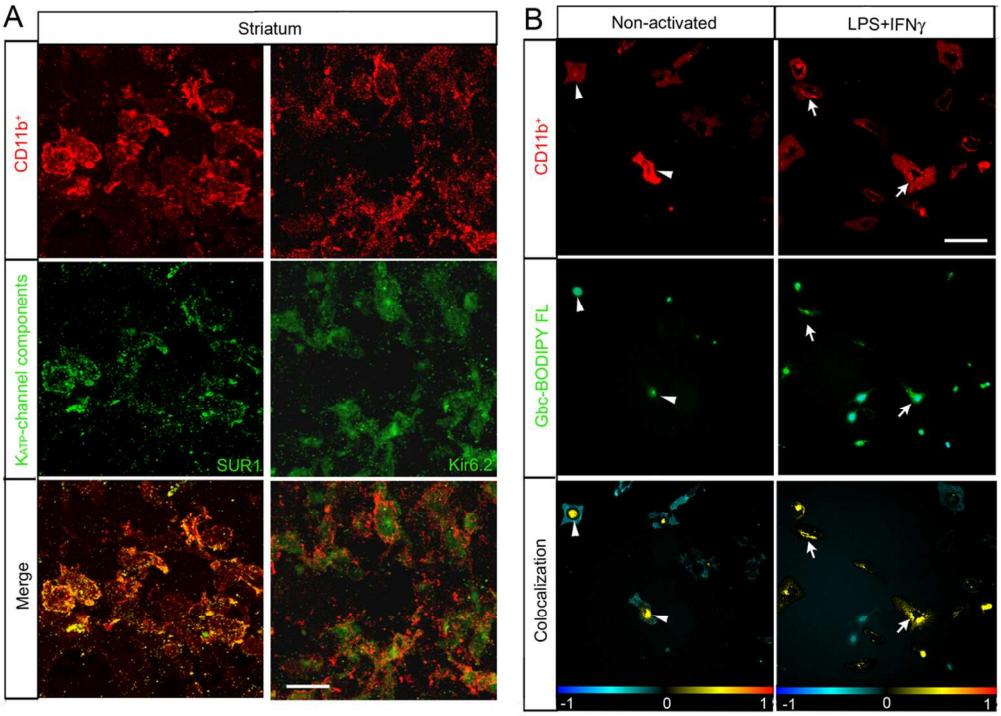

Figure 6. Reactive microglia express and translocate SUR1 to the cell surface. (A) Confocal photomicrographs of SUR1 and Kir6.2 (green) in reactive microglia (CD11b+; red) localized to the striatum adjacent to the ventricle in MCAO rats. Yellow in the merge image denotes colocalization, whereby reactive CD11b-postive cells expressed SUR1 or Kir6.2 seventy-two hours after ischemia. (B) Localization of glibenclamide (glibenclamide BODIPY FL; green fluorescence) in rat microglial primary culture. Non-activated or cultures activated with LPS+IFNγ for 48 h are shown in the upper row. Microglial cells were labeled with an anti-CD11b (red) antibody and Hoechst (blue) to stain the nuclei. Lower row shows respective colocalization of the red and green channels, where the yellow denotes the presence of the glibenclamide binding in microglial cells. Arrowhead denotes peri-nuclear colocalization and arrows show surface labeling; the data shown are representative of 4 experiments each. Scale bar in (A) is 15 μm and in (B) is 20 μm.
104x76mm (300 x 300 DPI)